Biochimica et Biophysica Acta, 978 (1989) 43–50
Elsevier

BBA 74263

The electrogenic proton/hexose carrier in the plasmalemma of *Chenopodium rubrum* suspension cells: effects of Δc, ΔpH and $\Delta\psi$ on hexose exchange diffusion

Johann Peter Gogarten * and Friedrich-Wilhelm Bentrup

Botanisches Institut I der Justus-Liebig-Universität, Giessen (F.R.G.)

(Received 7 June 1988)
(Revised manuscript received 4 October 1988)

Key words: Exchange diffusion; Photoautotrophic suspension cell; Proton/hexose cotransport; (*C. rubrum* L.)

The hexose carrier in the plasmalemma of a higher plant suspension cell (*Chenopodium rubrum* L.) catalyzes not only electrogenic proton/hexose symport, but also electroneutral exchange diffusion of hexoses. The transport process is studied mainly through short-term efflux disturbance of labelled 3-*O*-methyl-D-glucose (3-OMG). This novel method singles out the transport system in situ and reliably detects small (> 5%) changes of unidirectional hexose fluxes. The three driving forces for the electrogenic net uptake of hexose are the gradients of substrate (hexose), cosubstrate (H^+) and the electric potential difference across the plasmalemma. Increasing substrate concentrations (outside or inside) led to increased unidirectional fluxes into the compartment where the substrate concentration was increased (e.g., *trans* stimulation of 3-OMG efflux by external hexose); however, an increase of the external H^+ concentration at non-saturating external hexose concentrations led to a *trans* inhibition of 3-OMG efflux. Depolarization of the transmembrane electric potential difference without influencing the surface potential led to only a small increase in hexose efflux at low hexose concentrations and had no measurable effect at saturating hexose concentrations. However, depolarization mainly due to a decrease of the surface and Donnan potentials mimicked the effect of alkalinization. These findings agree with a model based on a negatively charged carrier showing random-order binding of substrate and cosubstrate on the outside of the plasmalemma. It is not necessary to assume a recycling translocation step of the empty substrate-binding site. The low-voltage sensitivity of the hexose efflux observed is discussed with regard to possible electric potential profiles at the site of transport.

Introduction

In 1977, Hüsemann and Barz [1] established a strictly photoautotrophically propagating suspension culture of *Chenopodium rubrum* L. However, these cells – like all higher and lower plant cells investigated so far – still have a very efficient sugar-uptake system. In their energy requirements and substrate specificity, these sugar-uptake systems are very similar to each other. Some of the differences observed between these uptake systems, in fact, may reflect differences in techniques and experimental conditions rather than differences inherent in the transport systems themselves. At the DNA level, substantial homologies exist between different species [2]. In most (if not all) plant cells, glucose is transported by an electrogenic proton symport (hydroxyl ion antiport) across the plasmalemma [3]. This is also true for cells from the photoautotrophic *Ch. rubrum* suspension cultures, having a maximal uptake rate of about 200 nmol (glucose for H^+ or charges) $\cdot$ $min^{-1} \cdot g_{FW}^{-1}$ which corresponds to about 5 $mA \cdot m^{-2}$ [4,5].

By employing the traditional method of compartmental analysis [6] to 3-*O*-methyl[^{14}C]glucose (3-[^{14}C]OMG) efflux experiments [7], it has been shown in situ that 3-OMG is transported across the plasmalemma into the cytoplasm and further transported across the tonoplast into the vacuole [5]. Even after short incubation times (< 1 h), the greatest part of the incorporated

* Present address: Thimann Laboratories, UCSC, Santa Cruz, CA 95064, U.S.A.

Abbreviations: 3-OMG, 3-*O*-methyl-D-glucose; ϕ_{XY} (ϕ^*_{XY}) = unidirectional flux (of tracer) (mol $\cdot$ $min^{-1} \cdot g_{FW}^{-1}$) from compartment X into Y; C, cytoplasm; V, vacuole; O, outside; s_x, specific radioactivity (dpm $\cdot$ mol^{-1}) in compartment x; Q_i^*, tracer content of compartment i (dpm/g_{FW}); FW, fresh weight; $\Delta\psi$: transmembrane difference in electric potential. Mes, 4-morpholineethanesulfonic acid.

Correspondence: F.W. Bentrup, Botanisches Institut I der Justus-Liebig-Universität, Senckenbergstrasse 17, 6300 Giessen, F.R.G.

3-OMG is found in the vacuole. This is because of the large size of the vacuole rather than due to uphill transport. This huge reservoir of intracellular 3-[^{14}C]OMG causes a large amplitude in the slow component of the efflux kinetics ($t_{1/2} \approx 5$ h). During this phase, the efflux can be disturbed repeatedly and reproducibly, since the cytoplasm is replenished with 3-[^{14}C]OMG from the vacuole [7]. This experimental approach has also been applied to studies of amino acid transport [8] and $K^+/^{86}Rb^+$ transport [9].

The concentration dependence of the *trans* stimulation of 3-OMG efflux by external hexose closely resembles the concentration dependencies found for hexose influx, hexose-induced proton uptake and membrane depolarization; the half-saturation constants are about 50 μM and 150 μM for D-glucose and 3-OMG, respectively [10,11]. By measuring the increase in energy consumption due to 3-OMG transport and the proton fluxes during *trans* stimulation of the 3-OMG efflux, it has been shown that the exchange diffusion giving rise to the *trans* stimulation does not dissipate the proton motive force across the plasmalemma. The energy invested during influx by a downhill flow of protons is regained during efflux.

In the present study, we investigate how the forces driving hexose uptake influence 3-OMG exchange diffusion. The results are used to discuss how and which part of the proton motive force across the plasmalemma (ΔpH and $\Delta\psi$) is sensed and transduced by the hexose carrier.

Material and Methods

Plant material and cell culture. The photoautotrophic suspension culture of *Ch. rubrum* L. [1] has been subcultured in our laboratory since 1979 (see Ref. 12 for detailed culture conditions). Prior to experiments, the suspension cells were incubated for at least 12 h in a test medium with the following composition: 2 mM NaCl, 0.1 mM KCl, 0.2 mM $CaCl_2$, 0.1 mM $MgCl_2$ and – if not stated otherwise – 2 mM NaH_2PO_4/Na_2HPO_4 buffer of pH 5.5. In this medium, without the use of a CO_2 buffer, the cells retain their viability for periods in excess of 6 days as measured by the phenosafranine or fluoresceindiacetate tests [12], and by the transport properties of the plasmalemma. Cells were harvested using gravity filtration through a 15 μm nylon mesh. Details of 1 g of harvested cells (FW) were (approx.): 20–25 mg_{DW}, $(5–10) \cdot 10^6$ cells, 0.05–0.1 m^2 cell surface, 0.5 ml vacuolar volume, 50 μl cytoplasmatic volume and 250 μg chlorophyll.

For experiments conducted with cells in suspension, cells were illuminated by white fluorescent light at 10 W/m^2 and incubated at 24–26 °C. Mixing of the suspension was achieved by a suspended magnetic stirrer or round-shaker with a frequency 20% greater than the minimum required for turbulent flow.

Radioactivity. This was measured by liquid scintillation counting using Unisolve 100 (Zinsser, Frankfurt/M, F.R.G.) in a Betamatic Scintillation Counter (Kontron, Zürich, Switzerland). Quench correction was calculated using the standard channel ratio. Cells were diluted with scintillation cocktail until the counting efficiency was greater than 45% as calculated from the channel ratio and quench polynomial.

Influx. 3-OMG influx was measured as the time course of appearance of radioactivity in the cells (0.2 g_{FW} in 10 ml medium) during the first 8.5 min after tracer addition (40 kBq, 30 TBq/mol) to the external medium (750 μM 3-OMG added at time zero). At 1.5-min intervals, 1 ml aliquots were taken and cells were separated from the medium by silicon-oil centrifugation [13] using a mixture of silicon oils AR 20 and DC 200 (Serva, Heidelberg, F.R.G.).

Metabolism of 3-OMG. Measurements were made as described in Ref. 7. After 6 days of incubation with 3-[U-^{14}C]OMG, 70% of the incorporated radioactivity was recovered as 3-OMG, 8% comigrated with sugar phosphates and 15% comigrated with sucrose. The only substance identified in the exit medium (exit = efflux without 3-OMG added to the medium) was 3-OMG.

Efflux. For efflux experiments, cells were preincubated in a test medium with added 3-[U-^{14}C]OMG. The cell density was 0.05–0.1 g_{FW}/ml, the specific radioactivity was adjusted so that the cells had incorporated at least 30 MBq/g_{FW} at the end of the loading period, from the original 33–270 MBq/g_{FW} added to the incubation medium at the beginning. 1 g_{FW} of cells was transferred into an efflux chamber. The efflux chamber was made from plexiglass similar to a short chromatography column with a diameter of 1.7 cm and a height of about 2.5 cm. The bottom consisted of a porcelain frit covered with a 15-μm nylon mesh. The cells were packed by gravity and by medium flow (about 1 ml/min, peristaltic pump P1, Pharmacia, Uppsala, Sweden). The cells were then covered with another circular nylon net to achieve a uniform flow through the cells. A head of about 1 ml medium was kept above the cells. At the beginning of the efflux, medium without labelled 3-OMG was pumped through the packed cells. The 3-OMG concentration in this medium (named standard efflux medium) was the same as that of the preincubation medium at the end of the loading period, but without radioactive label. In order to exclude local non-mixing spaces, the washing solution (efflux medium) was added drop-wise. Under these conditions, the cuvette kinetics (i.e., the exchange of tracer in the external medium, measured with L-sorbose and cellobiose, substances that are not transported into the cells) yielded a single time constant whose magnitude was inversely proportional to the speed of perfusion;

under the conditions of the experiments reported, the cuvette kinetics have a time constant of about 1 min [5]. The efflux medium was collected by a fraction collector at 1–5 min intervals. The radioactivity released from the cells was measured by liquid scintillation counting.

A given disturbance of the steady-state flux, i.e., of the slow component of the efflux kinetics when the cytoplasm gains as much radioactivity from the vacuole as it loses to the apoplast, was evaluated according to the following reasoning: immediately after the flux across the plasmalemma, ϕ_{CO}, changes to ϕ_{COd}, the specific radioactivity of the cytoplasm, $s_{C(i)}$, remains unchanged, the changed flux is thus directly mirrored by the change in radioactivity release, α:

$$\alpha = \frac{\phi^*_{COd} - \phi^*_{CO}}{\phi^*_{CO}} = \frac{(\phi_{COd} - \phi_{CO}) \cdot s_{C(i)}}{\phi_{CO} \cdot s_{C(i)}} = \frac{\phi_{COd} - \phi_{CO}}{\phi_{CO}}$$

where ϕ_{CO} and ϕ^*_{CO} denote the unidirectional flux of 3-OMG or radioactivity from the cytoplasm to the outside, respectively, $s_{C(i)}$ stands for the actual specific radioactivity in the cytoplasm and the index, d, denotes the same quantities immediately after onset of disturbance. Note that after prolonged disturbances, this equation does not hold; rather, the radioactivity release again approaches the steady-state net flux of radioactivity across the tonoplast, $\phi_{VC} - \phi_{CV}$, prior to the disturbance and, in fact, is independent of the fluxes across the plasmalemma.

Electrophysiological experiments were performed as described in Ref. 4.

Results

If, during an uptake measurement, the tracer is added after, rather than simultaneously with, the unlabelled substance, uptake of label does not mirror net uptake, but becomes a measurement of unidirectional influx. Fig. 1 shows this for uptake of 3-OMG. Clearly, the net uptake (slope of the curve giving the amount of intracellular 3-OMG) decreases with increasing intracellular concentration, i.e., from 74 to 25 nmol 3-OMG $\cdot$ min^{-1} $\cdot$ g_{FW}^{-1} within 60 min of incubation in 3-OMG; the opposite is true, however, for the measured unidirectional influx that increases by 45% with increasing cytoplasmic 3-OMG concentration, i.e. from 74 to 108 nmol $\cdot$ min^{-1} $\cdot$ g_{FW}^{-1}.

Stimulation of the 3-OMG efflux by external 3-OMG is shown in Fig. 2. Here, the 3-OMG concentration in the efflux medium is changed during the slow component of an efflux experiment which leads to an increased loss of radioactivity upon increase of the external concentration. This increase in radioactivity release upon stimulation is far in excess of that re-cycled by re-uptake during unstimulated efflux. Measurement of re-uptake by varying the rate of efflux chamber perfusion, that is, varying the concentration of radioactivity in the external medium without changing the 3-OMG concentration, showed that a hypothetical 100% *cis* inhibition of re-uptake would increase net radioactivity release by less than 21%.

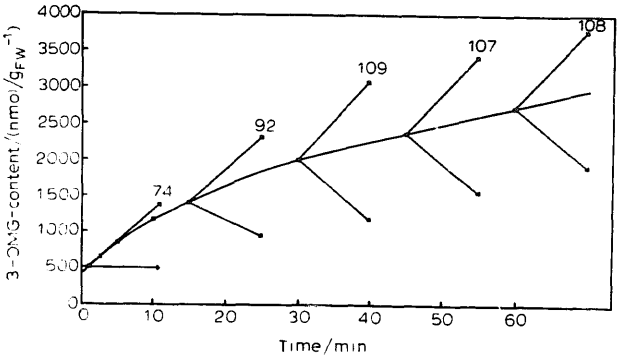

Fig. 1. Stimulation of 3-OMG influx by internal 3-OMG in suspension cells of *C. rubrum*. The curve gives the 3-OMG content in the suspension cells (0.2 g_{FW}/10 ml; initially 750 μM external 3-OMG) measured upon addition of tracer together with unlabelled 3-OMG. The slope of the curve represents the net rate of 3-OMG uptake. The upward arrows (slope and numbers given unidirectional influx in nmol $\cdot$ min^{-1} $\cdot$ g_{FW}^{-1}) were calculated from parallel experiments in which tracer was added at the times indicated by the origin of the arrows, i.e., after different times of preincubation with unlabelled 3-OMG. The unidirectional influx was calculated from the rate of increase of intracellular radioactivity and the external 3-OMG concentration at the time of tracer addition. The unidirectional efflux (downward arrows) was calculated from the difference between net uptake and unidirectional influx. The decrease in external 3-OMG was less than 7% after 1 h.

Acceleration of 3-OMG efflux by raising the external pH is demonstrated in Fig. 3. Obviously, at the non-saturating external 3-OMG concentration used in this experiment, the putative cosubstrate H^+ acts oppositely compared to the substrate. This effect is independent of the buffers used (Tris-Mes in Fig. 3 or phosphate in Fig. 4) and diminishes as the external 3-OMG concentration is increased: a pH shift from 6 to 7 stimulates 3-OMG

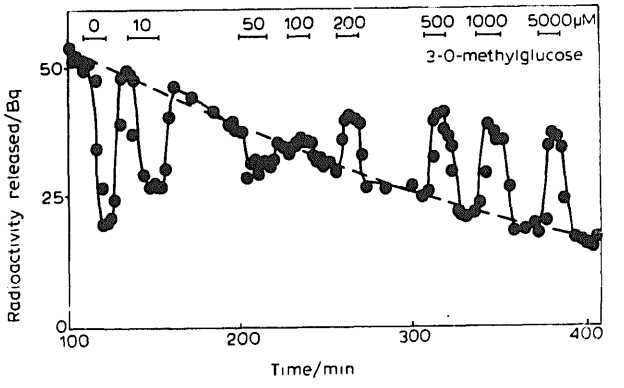

Fig. 2. Efflux kinetics showing *trans*- stimulation of 3-OMG efflux from *Chenopodium* suspension cells by the external 3-OMG. During the indicated time intervals, 3-OMG in the efflux medium was temporarily shifted from the standard concentration of 78 μM to the indicated values.

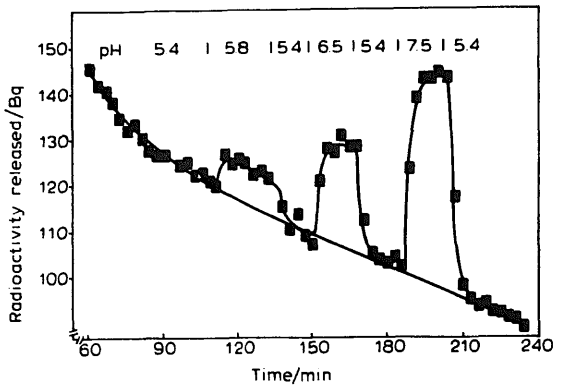

Fig. 3. *Trans* stimulation of 3-OMG efflux by transient increases in external pH. The efflux medium contained 150 μM 3-OMG and 4 mM Mes-Tris buffer to adjust the indicated pH values. Compartmental efflux analysis of the first 120 min at pH 5.4 yields $\phi_{CO} = 75$ nmol 3-OMG·min^{-1}·g$_{FW}^{-1}$.

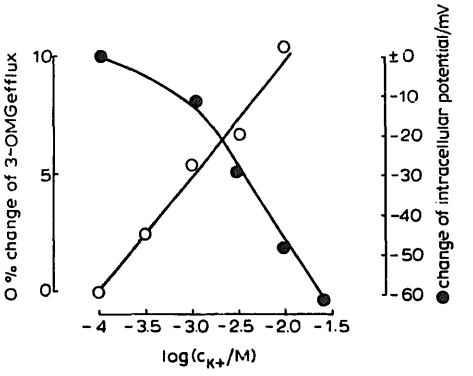

Fig. 5. Radioactivity release by 3-OMG efflux from a *Chenopodium* cell suspension (○, left ordinate), and intracellular electric potential of individual dark-adapted suspension cells (●, right ordinate) as a function of the external K^+ concentration (pH 6). The resting potential with 0.1 mM external K^+ is -165 (± 38) mV ($\pm$S.E., $n = 68$) [4]. Efflux medium: 1.5 μM 3-OMG and $c_{NaCl} + c_{KCl} = 10.1$ mM; electrophysiological measurement: $c_{NaCl} + c_{KCl} = 20.1$ mM.

efflux by about 260% at 15 μM external 3-OMG, by 80% at 57 μM and by only 15% at 150 μM, respectively. Instead, at saturating 3-OMG concentrations, a stimulation of 3-OMG efflux is observed at pH values below 5, if the proton concentration in the efflux medium is increased (Fig. 4).

The other driving force of the hexose carrier is the electric potential difference across the plasmalemma ($\Delta\psi$); this quantity can be varied by changing the medium's ionic composition. If Na^+ is exchanged for K^+, the difference in electric potential measured between cell interior and medium decreases by about 30 mV per 10-fold increase of external K^+ (Fig. 5). Since the ionic strength of the medium remains unchanged, this depolarization mainly reflects a smaller $\Delta\psi$ due to a changed diffusion potential. This balanced change in

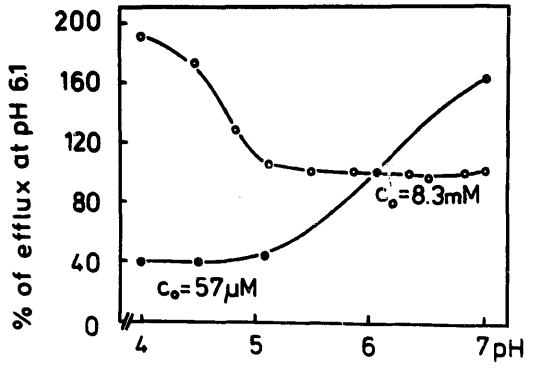

Fig. 4. pH dependency of 3-OMG efflux. The medium contained 10 mM phosphate buffer, the pH values given on the abscissa were measured in the efflux medium after passage through the efflux chamber. The ordinate gives the radioactivity release as a percentage of the radioactivity release at pH 6.1. From the compartmental analysis (using the first 120 min of undisturbed efflux), the unidirectional fluxes ϕ_{CO} at pH 6.1 were calculated to be about 50 nmol 3-OMG·min^{-1}·g$_{FW}^{-1}$ at 57 μM external 3-OMG and about 300 nmol 3-OMG·min^{-1}·g$_{FW}^{-1}$ at 8.3 mM 3-OMG (half-saturation of *trans*-stimulation occurs at an external concentration of 3-OMG of about 150 μM [5,11]).

K^+ concentration causes no reproducible effect on 3-OMG efflux at high (2 mM) external 3-OMG concentrations (the changes upon a 100-fold increase were smaller than $\pm 4\%$).

Changes in 3-OMG efflux at low external 3-OMG concentrations upon varying the K^+ concentration also

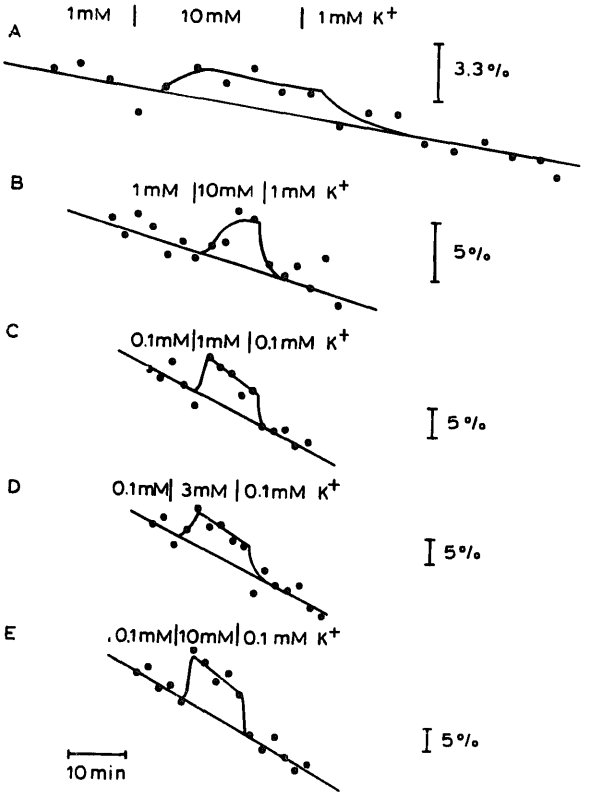

Fig. 6. Radioactivity release by 3-OMG efflux at low external concentration of 3-OMG upon transient changes in K^+ concentration (balanced by Na^+) as indicated. A, B, 30 μM 3-OMG; C, D, E, 1.5 μM 3-OMG. Medium: 2 mM Na_2HPO_4/NaH_2PO_4 buffer of pH 6; $c_{NaCl} + c_{KCl} = 10.1$ mM.

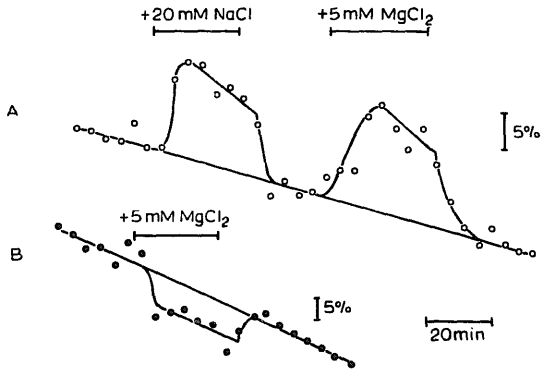

Fig. 7. Radioactivity release by 3-OMG efflux. Transient rise in ionic strength of the efflux medium depolarizing the surface potential of plasmalemma and the Donnan potential of the cell wall. Medium contained (A) 75 μM 3-OMG and (B) 712 μM 3-OMG.

are very small, but are reproducible (Fig. 6); at the same 3-OMG concentration, stimulation of radioactivity release (Fig. 5, left ordinate) increases with depolarization (Fig. 5, right ordinate).

On the other hand, if the ionic strength of the efflux medium was changed by addition of ions of low membrane permeability which, thus, mainly change the surface potential of the plasmalemma and the Donnan potential of the cell wall [14], a more pronounced effect could be observed (Fig. 7). At low 3-OMG concentrations, an increase in ionic strength leads to an increase in radioactivity release from the cells, at high 3-OMG concentrations, a slight decrease is observed under conditions that depolarize both the surface and Donnan potential.

Uptake of D-glucose did not respond to any kind of plasmalemma depolarization (10- to 100-fold increase of K^+ balanced by Na^+, addition of 20 mM NaCl or 5 mM $MgCl_2$) either at low or at saturating glucose concentrations (changes in uptake of more than 7% could have been detected).

Discussion

The high turnover of the exchange diffusion at the plasmalemma is clearly demonstrated in Figs. 1 and 2. The maximum measured turnover during this exchange diffusion was even higher than the turnover during influx with very low (or zero) *trans* substrate concentrations (Fig. 1). However, the influx with no 3-OMG on the *trans* side (time zero in Fig. 1) might be underestimated, because the incoming radioactivity is not washed away with a high volume of medium, as in the case of efflux measurements, nor is the specific radioactivity lowered by non-labelled 3-OMG that is already present on this side. Thus, in the case of low cytoplasmic 3-OMG concentrations, the efflux of label may lower the measured quantity.

It has been postulated that a high level of exchange diffusion is a general feature of hexose transport in plant cells and, possibly, of other transport systems with substrates which are rapidly metabolized under physiological conditions [15].

If exchange diffusion with saturating hexose concentrations on the respective *trans* side shows a higher turnover than uptake with zero hexose concentration on the *trans* side, the unidirectional flux is stimulated by the presence of substrate on the *trans* side. It is now demonstrated that this *trans* stimulation of the unidirectional hexose flux, that previously has been described for *Chlorella* [16,17] and *Riccia* [7], also exists in hexose transport across the plasmalemma of a higher plant (Fig. 2). This *trans* stimulation was found for 3-OMG efflux (Fig. 2), and probably is also present for influx (Fig. 1), although to a lesser extent. We found no indication for *trans* inhibition of 3-OMG uptake contrary to the assumed generalization of *trans* inhibition of 'sugar' influx [3].

On the level of reaction kinetics, this *trans* stimulation of a given efflux is plausible, if immediate transmembrane re-cycling of the empty binding site to the cytosolic side takes more time than its re-cycling via the following three minimum steps: (a) substrate loading on the apoplastic side; (b) its subsequent translocation (probably only a conformational change in the transporter molecule allowing substrate access) to the other side; and (c) unloading of the unlabeled substrate.

Taken individually, all of the results observed can be explained by the different possible six-state models for transport cycles [18]; however, we were not able to find a single six-state model that could explain simultaneously all of the following results.

Trans stimulation of influx and efflux (maximally approx. 400%) by the substrate.

Trans inhibition of efflux by the cosubstrate at a non-saturating substrate concentration.

No effect or *trans*-stimulation of the cosubstrate at saturating substrate concentrations.

Approx. the same half-saturation constants for influx and *trans* stimulation of efflux.

The same order of magnitude for maximal unidirectional influx and exchange diffusion ($\Delta pH \approx 2.5$, $\Delta\psi \approx -150$ mV).

Our search of the possible state space (eight possible carrier cycles corresponding to four different loading and unloading sequences of either a neutral or a negatively charged transporter with no a priori constraints on the relative magnitude of the reaction constants) is far from complete, thus our inability to find an appropriate six-state model does not prove that none exist.

Although an eight-state model with random-order binding is more complicated as far as the number of states of the transport system and, thus, the complexity of the mathematical treatment is concerned, the following features make it conceptually more appealing.

As all possible binding sequences are embedded in a

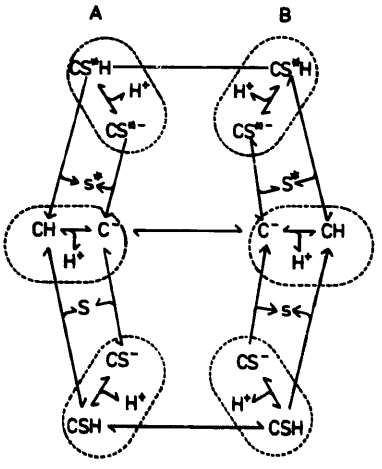

Fig. 8. Reaction kinetic eight-state model of a transport system with random-order binding of substrate and cosubstrate under counterflow conditions. The labelled substrate (S^*, higher; s^*, lower concentration) is transported from one side of the membrane (B) to the other (A). When re-cycling of the binding site via C^- is slower than that via the ternary complex CSH, addition of unlabelled substrate S on side A *trans* stimulates the flux of S^* from B to A. Note that a counter exchange can be catalyzed without participation of the state C^-. See text.

single model, it is not necessary to select from the four different possible orders of substrate and cosubstrate binding.

All six-state models with a kinetically (as opposed to sterically) controlled binding order are equally well represented by the random-order binding scheme.

Thus, although we did not find any deviation in *Chenopodium* from a single Michaelis-Menten type kinetics for hexose influx (10 μM to 10 mM substrate concentration), which has often been reported for sugar-uptake measurements (reviewed in Ref. 3) and which could be taken as indicative of random-order binding [19], we tested this binding scheme for its explanatory potential.

The observation that the cosubstrate *trans* inhibits 3-OMG efflux at non-saturating 3-OMG concentrations (Figs. 3 and 4), suggests that either the increased proton concentration interferes with the unloading of labelled substrate on the outside or that there at least one state of the transporter exists which becomes more populated as the outside proton concentration is increased and which is slow in forming the translocated ternary complex CSH. The latter sequence of events is embedded in the random-order binding scheme of Fig. 8; it holds if the reaction $CH + S \rightarrow CSH$ on the outside is sufficiently slow or non-existent. The assumption that this slow or 'dead-end' protonated state indeed reflects the transporter without bound substrate is supported by the fact that the observed *trans* inhibition by H^+ diminishes with rising substrate concentration; namely, if substrate is bound to the binding site, protonation fails to decrease the efflux. Conversely, with saturating substrate concentrations and a pH < 5, 3-OMG efflux increases with rising H^+ concentrations (Fig. 4). Thus, although the possibility cannot be ruled out that the observed stimulation of 3-OMG efflux by external H^+ (< 100%) is brought about by indirect effects (e.g., via changing concentration of $H_xPO_4^{(3-x)}$ ions), the reversible stimulation observed fits nicely into the proposed random-order binding scheme.

To our surprise, the *trans* stimulation of 3-OMG efflux by the external substrate concentration could still be modelled if the transmembrane re-cycling step ($C_i^- \rightarrow C_o^-$ in Fig. 8) was assumed to be very fast, thus apparently contradicting the explanation given above for *trans* stimulation. Considering a transporter, however, with more than one state with an empty binding site oriented to the outside medium (such as C^- and CH in Fig. 8), only probabilities can be compared for the two translocation pathways via translocation of C^- or via CSH, respectively, translocating from the external pool of all states with empty binding sites ($[C_o^- + CH_o]$) to the cytoplasmic one ($[C_i^- + CH_i]$). The probability for the translocation of the empty binding site may be low, not because of the small rate constant for translocation, but because the main subpopulation of substrate-binding sites consists of states that do not translocate to the other side of the membrane (if, for example, $[CH] > [C^-]$ in Fig. 8).

Note that *trans* stimulation still could be observed, even when the rate constant for translocation of the empty substrate-binding site increased indefinitely, that is, when the populations of C^- on membrane sides A and B, form a single population! A transmembrane shuttle movement of a substrate-binding site, therefore, is no cogent mechanism for a carrier sensu strictu, as in the case of a cotransporter showing *trans* stimulation. Categorically, our results suggest that the distinction between a carrier and a pore (or channel) is elusive.

Transmembrane voltage effects and profile

Depolarization of the diffusion potential failed to affect the 3-OMG efflux significantly at high external 3-OMG concentrations, i.e., by less than 4% at 2 mM 3-OMG. Thus, either the voltage-dependent step(s) are completely isolated from the limiting step by reaction steps being far from equilibrium or, more likely, the counter exchange of 3-OMG is catalyzed without a voltage-dependent step being involved. The latter explanation implies, that the translocated ternary complex CSH is neutral and that the hexose-induced net inward flow of positive charge of 7.5 $mA \cdot m^{-2}$ [5] must be coupled to the outward re-cycling of the empty binding site C^-. In accordance with this view of a negatively charged empty binding site, radioactivity release during 3-OMG efflux at low (micromolar) external 3-OMG concentrations is slightly increased by membrane depolarization (Fig. 5 and 6), corresponding to increased

inward re-cycling of the empty binding site. Note that from the data presented the possibility cannot be excluded that this slight increase in radioactivity release is due to a decrease in re-uptake of already released labelled 3-OMG. In an electrophysiological study on *Riccia fluitans*, Felle [20] has proposed a negatively charged proton/amino acid cotransporter. A negatively charged carrier also was proposed by Reinhold and Kaplan [3] because of the relative magnitudes of efflux and counterflow, respectively.

Quantitatively, however, the asymmetry between influx and maximal efflux on one hand, and 'efflux' (exit) in the absence of external hexose on the other (Fig. 2; maximal efflux ≈ 4-fold exit) is smaller than might be expected if the charge of the empty binding site during translocation would move all the way along the measured membrane potential (−150 to −200 mV; if one assumes a symmetrical energy barrier for the charge translocation, the reaction constant that describes the downhill translocation of an elementary charge is larger than that for the uphill translocation by a factor of $\exp(F \cdot \Delta\psi/(R \cdot T))$ [21]. With $\Delta\psi = 180$ mV, this would give a ratio of approx. 10^3; however, this charge transfer reaction can be more or less isolated from the rate-limiting step under the experimental conditions by reactions that are far from equilibrium [18]). Since conditions depolarizing the plasmalemma surface potential and the cell wall Donnan potential markedly influence 3-OMG efflux (Fig. 7) and, secondly, since this influence simulates alkalinization (i.e., increases efflux at low external 3-OMG concentration and decreases it at high external 3-OMG concentrations), the measured membrane potential ($\Delta\psi$) could be partly converted by surface and Donnan potentials, respectively, into an increased H^+ concentration gradient (Fig. 9). The electrochemical potential of H^+ outside the plasmalemma remains constant, since the more negative electrical potential would be balanced by the corresponding increase in H^+ concentration. This interconversion of $\Delta\psi$ into an increased ΔpH has also been postulated in Harold's description [22] of the proton-well theory for F_oF_1-ATPases [23]. To reiterate a conclusion drawn from Harold's discussion of the binding order: the experimental results can be accounted for even in the extreme case in which the empty binding site and the charge are not transported across the membrane, i.e., if there was only one pool of carriers without bound substrate and cosubstrate; in this case, either the binding site is in a region of locally very high surface potential or (and) the proton-accepting site has a high-resistance access channel (i.e., the high-field access channel suggested by Läuger and Jauch [24]).

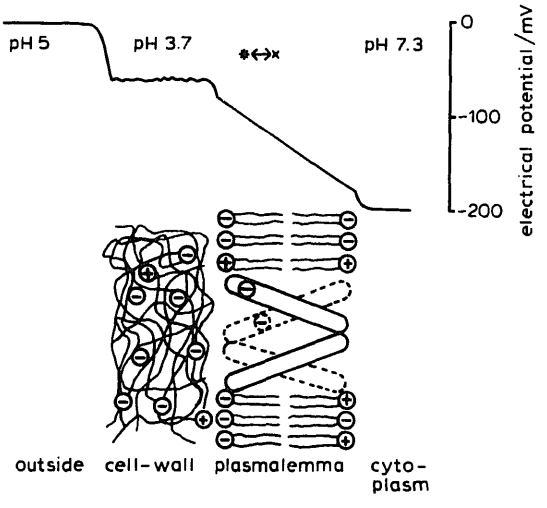

Fig. 9. Top: tentative profile of the electrical potential between cytoplasm and external medium ($\Delta\psi$). Bottom: scheme of cell wall and plasmalemma with hexose transporter. The double-headed arrow above the potential profile denotes the small fraction of the voltage profile experienced by the transporter's charge during translocation. See text.

Acknowledgements

The late Soehadi Noersingghi devotedly reared the *Chenopodium* cultures. We are grateful to Susanne Tröster for expert technical assistance, and we acknowledge the valuable suggestions made by M. Gogarten-Boekels and C.L. Slayman. This work was supported by a grant from the Deutsche Forschungsgemeinschaft (Be 466/21-3).

References

1 Hüsemann, W. and Barz, W. (1977) Physiol. Plant 40, 77–81.
2 Maiden, M.C.J., Davis, E.O., Baldwin, S.A., Moore, D.C.M. and Henderson, P.J.F. (1987) Nature 325, 641–643.
3 Reinhold, L. and Kaplan, A. (1984) Annu. Rev. Plant Physiol. 35, 45–83.
4 Ohkawa, T.A., Köhler, K. and Bentrup, F.-W. (1981) Planta 151, 88–94.
5 Gogarten, J.P. (1986) Untersuchungen zum Zuckertransport an Photoautotrophen Suspensionszellen von *Chenopodium rubrum* L. Ph.D. Thesis, Giessen.
6 Walker, N.A. and Pitman, M.G. (1976) in Encyclopedia of Plant Physiology, New Series, Vol. 2A (Lüttge, U. and Pitman, M.G., eds.), pp. 93–124, Springer, Berlin.
7 Gogarten, J.P. and Bentrup, F.-W. (1983) Planta 159, 423–431.
8 Felle, H. (1984) Analyse von Primär und Sekundär Aktiven Transportmechanismen am Plasmalemma von *Riccia fluitans* mit Besonderer Berücksichtigung Chemiosmotischer Zusammenhänge. Habilitationsschrift, Giessen.
9 Dahse, I., Felle, H., Bentrup, F.-W. and Liebermann, B. (1986) J. Plant Physiol. 124, 87–93.
10 Gogarten, J.P. and Bentrup, F.-W. (1984) in Membrane Transport in Plants (Cram, W.J., Janácek, K., Rybová, R. and Sigler, K., eds.), pp. 183–188, Academia Publishing House, Praha.
11 Bentrup, F.-W. (1985) Naturwissenschaften 72, 169–179.
12 Gogarten-Boekels, M., Gogarten, J.P. and Bentrup, F.-W. (1985) J. Plant Physiol. 118, 309–325.
13 Werdan, K., Held, H.W. and Geller, G. (1972) Biochim. Biophys. Acta 283, 430–441.

14 Gogarten, J.P. (1988) Planta 174, 333–339.
15 Sauer, N., Komor, E. and Tanner, W. (1983) Planta 159, 404–410.
16 Komor, E., Haas, D. and Tanner, W. (1972) Biochim. Biophys. Acta 266, 649–666.
17 Komor, E., Haas, D., Komor, B. and Tanner, W. (1973) Eur. J. Biochem. 39, 193–200.
18 Sanders, D., Hansen, U.-P., Gradmann, D. and Slayman, C.L. (1984) J. Membr. Biol. 77, 123–152.
19 Sanders, D. (1986) J. Membr. Biol. 90, 67–87.
20 Felle, H. (1984) Biochim. Biophys. Acta 772, 307–312.
21 Schultz, S.G. (1980) in: Basic Principles of Membrane Transport, p. 109, Cambridge University Press, Cambridge.
22 Harold, F.M. (1986) The Vital Force; A Study of Bioenergetics, p. 239, W.H. Freeman and Company, New York.
23 Mitchell, P. (1976) Biochemical Society Transactions 4, 399–430.
24 Läuger, P. and Jauch, P. (1986) J. Membr. Biol. 91, 257–284.